MCB
Journals.ASM.org

Defective Mitochondrial Morphology and Bioenergetic Function in Mice Lacking the Transcription Factor Yin Yang 1 in Skeletal Muscle

Sharon M. Blättler,[a,b] Francisco Verdeguer,[a,b] Marc Liesa,[c] John T. Cunningham,[a,b] Rutger O. Vogel,[a,b] Helen Chim,[a,b] Huifei Liu,[b] Klaas Romanino,[d] Orian S. Shirihai,[c] Francisca Vazquez,[a,b] Markus A. Rüegg,[d] Yang Shi,[b] and Pere Puigserver[a,b]

Department of Cancer Biology, Dana-Farber Cancer Institute,[a] Department of Cell Biology, Harvard Medical School,[b] and Department of Medicine, Mitochondria ARC, Evans Biomedical Research Center, Boston University School of Medicine,[c] Boston, Massachusetts, USA, and Department of Neurobiology, Biozentrum, University of Basel, Basel, Switzerland[d]

The formation, distribution, and maintenance of functional mitochondria are achieved through dynamic processes that depend strictly on the transcription of nuclear genes encoding mitochondrial proteins. A large number of these mitochondrial genes contain binding sites for the transcription factor Yin Yang 1 (YY1) in their proximal promoters, but the physiological relevance is unknown. We report here that skeletal-muscle-specific YY1 knockout (YY1mKO) mice have severely defective mitochondrial morphology and oxidative function associated with exercise intolerance, signs of mitochondrial myopathy, and short stature. Gene set enrichment analysis (GSEA) revealed that the top pathways downregulated in YY1mKO mice were assigned to key metabolic and regulatory mitochondrial genes. This analysis was consistent with a profound decrease in the level of mitochondrial proteins and oxidative phosphorylation (OXPHOS) bioenergetic function in these mice. In contrast to the finding for wild-type mice, inactivation of the mammalian target of rapamycin (mTOR) did not suppress mitochondrial genes in YY1mKO mice. Mechanistically, mTOR-dependent phosphorylation of YY1 resulted in a strong interaction between YY1 and the transcriptional coactivator peroxisome proliferator-activated receptor gamma coactivator 1α (PGC1α), a major regulator of mitochondrial function. These results underscore the important role of YY1 in the maintenance of mitochondrial function and explain how its inactivation might contribute to exercise intolerance and mitochondrial myopathies.

Mitochondrial organelles are dynamic tubular or rounded structures in the cytoplasm largely devoted to nutrient metabolism and bioenergetics. The size, integrity, and location of mitochondria are controlled through different protein-regulated processes that depend on timely, adequate transcriptional control of nuclear genes encoding mitochondrial proteins (16, 18, 20, 25, 29, 35). These mitochondrial processes are regulated in response to different bioenergetic demands to maintain cellular energy homeostasis. At the tissue level, proper mitochondrial function is essential for adaptation to different physiological conditions, for example, to energetic demands in skeletal muscle during exercise (9, 23). Notably, dysregulation of mitochondrial processes is associated with a broad array of diseases, including myopathies and neurodegeneration, underscoring the importance of intact mitochondrial activities in human health (8, 41).

Mitochondrial structural and functional processes depend strictly on a continuous, regulated supply of mitochondrial proteins, initially provided by the activities of transcriptional components bound to the promoters of nuclear mitochondrial genes. Two different families of transcription factors play a pivotal role in the control of mitochondrial genes: the nuclear respiratory factors (NRF1 and NRF2) and the nuclear hormone estrogen-related receptors (ERRα, ERRβ, and ERRγ) (11, 28). Interestingly, the activity of these transcriptional factors is strongly amplified by the expression of the peroxisome proliferator-activated receptor gamma coactivator 1 (PGC1) family of coactivators, which includes PGC1α, PGC1β, and PRC (12, 14, 34). The assembly of these transcription factors and PGC1 coactivators ensures the robust induction of a full program of gene expression necessary for all facets of mitochondrial function: biogenesis, cellular distribution, and bioenergetic activity. For example, tissue-specific transgenic expression of PGC1α in skeletal muscle is sufficient to fully convert muscle fibers from type 2 fast-twitch to type 1 slow-twitch fibers with high mitochondrial content (22). Furthermore, PGC1α transgenic mice are largely protected against several mitochondrial myopathies and age-associated diseases (43, 44).

Using computational genomics, we determined previously that a large number of nuclear mitochondrial genes activated by PGC1α contained DNA binding sites for the transcription factor YY1 (10). YY1 binds DNA through four C-terminal zinc finger domains and can function as an activator or repressor of gene expression (31, 49). Within the context of mitochondrial genes, YY1 physically interacts with and recruits PGC1α to target promoters. From a regulatory standpoint, the interaction between these two proteins is dependent on mammalian target of rapamycin (mTOR) activity, but the molecular mechanisms accounting for this interaction are unknown. Interestingly, mTOR controls mitochondrial gene expression, and a deficiency of mTOR or the mTOR complex 1 (mTORC1) component raptor in skeletal muscle-specific knockout (KO) mice results in a profound mitochondrial dysregulation associated with dystrophy (4, 32). These mouse phenotypes are exactly the opposites of those described

Received 15 March 2012 Returned for modification 16 April 2012
Accepted 9 June 2012
Published ahead of print 18 June 2012
Address correspondence to Pere Puigserver, Pere_Puigserver@dfci.harvard.edu.
Supplemental material for this article may be found at http://mcb.asm.org/.

doi:10.1128/MCB.00337-12

above for the skeletal muscle PGC1α transgenic mice and support convergence of this signaling/transcriptional pathway. Despite the fact that YY1 was placed in this pathway, the precise role of YY1 in skeletal muscle mitochondrial physiology *in vivo* and the way in which it impacts physiopathology at the tissue and whole-body levels are unknown.

We report here that specific YY1 deficiency in skeletal muscle results in profound mitochondrial dysregulation, exercise intolerance, and signs of myopathy causing attenuated postnatal growth and short stature. Skeletal-muscle-specific YY1 knockout (YY1mKO) mice contained a decreased number of mitochondria with severe morphological defects, including poorly formed cristae and accumulation of intramitochondrial aggregates. Moreover, mitochondria were disorganized and mislocalized in the myofiber architectural structure. This phenotype was consistent with a strong decrease in mitochondrial gene expression that resulted in bioenergetic deficiencies. Interestingly, YY1mKO mice were insensitive to the suppressive effects of the mTOR inhibitor rapamycin on mitochondrial genes. Molecularly, mTOR-dependent phosphorylation of YY1 led to interaction with PGC1α and increased mitochondrial gene expression. These results support an important functional role of YY1 in maintaining skeletal muscle mitochondrial morphology and bioenergetic state, and they indicate that YY1 inactivation results in a phenotype that resembles mitochondrial diseases.

MATERIALS AND METHODS

Constructs and reagents. YY1 and YY1 short hairpin RNA (shRNA) adenoviral constructs have been described previously (10). YY1 site-directed mutations were made using QuikChange site-directed mutagenesis (Stratagene). The antibodies used were anti-YY1 (Santa Cruz catalog no. 281), anti-PGC1α (Santa Cruz catalog no. 13067), antitubulin (Upstate catalog no. 05-661), antiporin (Mitoscience catalog no. MSA03), anti-succinate dehydrogenase complex, subunit A (anti-SDHA; Mitoscience catalog no. MS204), anti-ATPase α (Mitoscience catalog no. MS502), anti-Core II (Mitoscience catalog no. MS304), anti-Ndufa9 (Mitoscience catalog no. MS111), anti-Ndufs3 (Mitoscience catalog no. MS110), and anti-Cox5a (Mitoscience catalog no. MS409).

Generation of YY1mKO mice. YY1mKO mice were generated by breeding animals harboring a floxed YY1 allele (1) with mice that transgenically express *cis*-acting replication element (CRE) recombinase under the control of the myogenin promoter and the MEF2C enhancer (19). Wild-type littermates carrying the floxed allele but not CRE were used as a control group. These mice have a mixed background.

Animal experiments. All experiments and protocols were approved by the Institutional Animal Care and Use Committee of the Dana-Farber Cancer Institute or Beth Israel Deaconess Medical Center. Mice were housed on a 12-h:12-h light-dark cycle (lights on at 6 a.m.). Mice were allowed *ad libitum* access to standard laboratory rodent chow. The fat and lean tissue masses in living, nonanesthetized mice were determined by using magnetic resonance imaging (MRI) equipment (Echo Medical Systems, Houston, TX). Six-week-old YY1mKO males and wild-type littermates were injected daily intraperitoneally at 5 p.m. with 2.5 mg/kg of body weight rapamycin or a vehicle (0.1% dimethyl sulfoxide [DMSO] in sterile phosphate-buffered saline [PBS]). Mice with free access to food and water were sacrificed 12 h after final rapamycin/vehicle injection (5 a.m.). Twelve-week-old raptor knockout (RamKO) males and wild-type littermates were injected daily intraperitoneally at 5 p.m. with 2.5 mg/kg rapamycin or a vehicle (0.1% DMSO in sterile PBS). Mice with free access to food and water were sacrificed 12 h after final rapamycin/vehicle injection (5 a.m.).

Exercise performance. Six-month-old mice were run on a motorized, speed-controlled, modular treadmill system (Columbus Instruments). The treadmill was equipped with an electric shock stimulus. Mice were acclimatized to the treadmill for a week (10 min/day); then either the mice were time/distance run to exhaustion or the number of stops within 10 min was recorded. For the experiment to exhaustion, mice were run at 5 m/min for 5 min, and then the speed was increased every 5 min up to 20 m/min (in 5-m/min steps). For the stop count, they were run at 10 m/min for 10 min, and then the number of falls into the motivational grid was counted for an additional 10 min. For voluntary exercises, mice were housed individually in cages containing a running wheel (Bio-Serv, Frenchtown, NJ) for 6 days, and their running activity was monitored.

Histology and EM. For electron microscopy (EM) analyses, adult mice were euthanized, and muscle tissue was rapidly fixed with Karnovsky's fixative (2% glutaraldehyde, 1% paraformaldehyde, and 0.08% sodium cacodylate). Muscle was dissected, postfixed in 1% osmium tetroxide, dehydrated in graded ethanol, embedded in Poly-Bed plastic resin, and sectioned for EM. EM was performed by the Harvard Medical School Electron Microscopy core facility. For hematoxylin and eosin (H&E) staining, mice were euthanized and were rapidly fixed in Bouin's fixative. Muscle tissue was formalin fixed, embedded in paraffin, sectioned, and stained with H&E and Masson's trichrome. For SDH, cytochrome oxidase (COX), and periodic acid-Schiff stain (PAS) staining, muscle tissue was frozen in isopentane that had been cooled in liquid nitrogen. Staining was performed by the Specialized Histopathology Service using standard protocols for these assays (Longwood, Boston, MA).

Cell culture and treatments. C_2C_{12} cells were cultured in Dulbecco's modified Eagle medium (DMEM) containing 10% fetal bovine serum. C_2C_{12} myoblasts were differentiated in DMEM with 2% horse serum for 72 h before infection with the indicated adenoviral constructs. Forty-eight- to 72-h-infected C_2C_{12} myotubes were treated with 20 nM rapamycin or a vehicle for 16 h.

Gene expression analysis. RNA was isolated by TRIzol (Invitrogen), reverse transcribed using SuperScript II reverse transcriptase, and analyzed by quantitative real-time PCR (qRT-PCR) with SYBR green fluorescence. Primer sequences are available upon request. Cell culture data were normalized to β-actin expression. Mouse data were normalized to 2-beta-mercaptoethanol (2-βM) expression, and RNA was extracted from the skeletal muscles of fed mice. A list of qRT-PCR primer sequences is provided in Fig. S5 in the supplemental material.

ChIP. Cells were fixed in 1% formaldehyde–serum-free DMEM for 10 min at 37°C. Cross-linking was then quenched in 0.150 M glycine, and cells were washed twice in PBS. Cells were collected in chromatin immunoprecipitation (ChIP) buffer (50 mM HEPES, 140 mM NaCl, 1 mM EDTA, 1% Triton, 0.1% sodium deoxycholate [NaDOC], 0.1% sodium dodecyl sulfate [SDS] with fresh protease inhibitors). Samples were sonicated 6 times with a duty cycle of 30 s on/30 s off, and 10 μg of DNA was immunoprecipitated (16 h) with either 2 μg of YY1 antibody (sc-281; Santa Cruz) or IgG. Immunocomplexes were recovered with protein A Dynabeads (100-02D; Invitrogen) and were washed 6 times. DNA was de-cross-linked, purified, and then quantified by qPCR. Mice ($n = 4$) were first treated with a vehicle or with 2.5 mg/kg rapamycin for 2 weeks, then fasted for 16 h, and finally refed for 6 h before sacrifice. Two gastrocnemius muscles of each mouse were dissected, cut in pieces, and fixed in 1% formaldehyde-PBS for 15 min at room temperature. The fixation was quenched by adding a final concentration of 0.150 M glycine, and muscle pieces were washed twice in cold PBS. The tissue was homogenized in cold PBS (containing protease inhibitors) in a motor pestle. The homogenate was filtered in 100-μm-pore-size cell strainers and was pelleted by centrifugation for 5 min at 4,000 rpm and 4°C. The pellet was resuspended in 500 μl SDS lysis buffer from the Millipore EZ-ChIP kit. Samples were sonicated in a Diagenode Bioruptor for 5 duty cycles of 30 s on/30 s off and were finally centrifuged for 15 min at 10,000 × *g*. Fifty microliters of each sample was diluted 1:10 in dilution buffer (from the EZ-ChIP kit) and was incubated overnight at 4°C with 2 μg of an anti-YY1 antibody (sc-281X;

Santa Cruz) or IgG, respectively. Immunocomplexes were recovered with protein A Dynabeads (100-02D; Invitrogen). Finally, DNA was purified and quantified by qRT-PCR. A list of qRT-PCR primer sequences is provided in Fig. S5 in the supplemental material.

Immunoprecipitation and Western blot analysis. Total-protein extracts from cells or tissues were prepared in a buffer containing 20 mM HEPES (pH 7.9), 125 mM NaCl, 0.3% 3-[(3-cholamidopropyl)-dimethylammonio]-1-propanesulfonate (CHAPS), 10 mM pyrophosphate, 1 mM EDTA, protease inhibitors, and phosphatase inhibitors. YY1 was immunoprecipitated by anti-YY1 antibodies or Flag beads as indicated in the figure legends, and the interaction with PGC1α was detected by specific antibodies. All Western blotting with the indicated primary antibodies was performed by overnight incubation at 4°C.

Transient-transfection and luciferase reporter assays. Transient transfection was performed in HEK-293 cells using Polyfect (Qiagen) at a DNA/Polyfect ratio of 1:2. The cell culture medium was changed after 12 h, and rapamycin was added (20 nM). Cells were lysed with Reporter Lysis buffer (Promega) 36 h after transfection, and luciferase assays were performed with the Dual-Glo luciferase assay system (Promega).

GSEA. Gene expression microarrays of total RNA from the solei of 6-month-old YY1mKO mice or wild-type littermates were performed by the Microarray Core at the Dana-Farber Cancer Institute using an Affymetrix GeneChip Mouse Genome 430A 2.0 array. CEL files were processed with the Expression File Creator module from Gene Pattern (http://genepattern.broadinstitute.org) using the default parameters, and the output file was used as input for gene set enrichment analysis (GSEA) (37). We ran GSEA, version 2.0, using the default parameters but changing the permutation type to gene set and using MSIGDB collection C2 (curated gene sets), version 3.0.

Mitochondrial isolation and respirometry. Gastrocnemius muscles (both legs) were homogenized on ice using a Wheaton glass-to-glass Dounce homogenizer (30 strokes) in ice-cold mitochondrion isolation buffer for muscle (9a) (100 mM KCl, 50 mM morpholinepropanesulfonic acid [MOPS], 1 mM EDTA, 5 mM $MgSO_4$, 1 mM ATP [pH 7.4] with bacterial proteinase from Sigma [P8038] at 0.3 mg/g tissue) after a 5-min incubation at room temperature. The homogenate was diluted 1/2 in modified mitochondrion isolation buffer (with 0.2 mM ATP and 0.5% fatty-acid-free bovine serum albumin [BSA]) and was centrifuged at 600 × *g* for 10 min at 4°C. The pellet was discarded and the supernatant centrifuged at 10,000 × *g* for 10 min at 4°C. The mitochondrial pellet was washed once with the modified buffer and once with the mitochondrial isolation buffer (10 min at 10,000 × *g* for each wash). The pellet was resuspended in HES buffer (pH 7.4) (5 mM HEPES, 1 mM EDTA, 0.25 M sucrose) and was kept on ice, and protein was quantified using a bicinchoninic acid (BCA) assay from Pierce. Respirometry was performed using the XF24-3 platform from Seahorse Biosciences, as described previously (21, 33). Briefly, 12.5 μg of protein (3 to 6 μl) was loaded at the center of the V7 plate on ice, and 50 μl of the substrates (5 mM pyruvate plus 5 mM malate in mitochondrial assay solution [MAS] [pH 7.4]) and 440 μl of MAS (70 mM sucrose, 220 mM mannitol, 5 mM KH_2PO_4, 5 mM $MgCl_2$, 2 mM HEPES, 1 mM EGTA, and 0.2% BSA [pH 7.4]) were carefully added on top. All the chemicals loaded in the Seahorse cartridge ports were diluted in MAS, and the pH was adjusted to 7.4. State 3 was induced by 1 mM ADP with 5 mM pyruvate plus 5 mM malate (port A), state 4o by 2 μM oligomycin (complex V/ATP synthase inhibitor), and uncoupled respiration by 4 μM carbonyl cyanide *p*-trifluoromethoxyphenylhydrazone (FCCP). Antimycin A (4 μM) was used to control background, nonmitochondrial respiration. C_2C_{12} myoblasts were grown and differentiated in a Seahorse plate. Basal respiration was followed, and then maximal respiration and nonmitochondrial respiration were measured by addition of FCCP (3 μM) and rotenone (2 μM).

BN-PAGE analysis. Native protein lysates for blue native polyacrylamide gel electrophoresis (BN-PAGE) analysis were obtained by dissolving the PBS-washed cell pellet in a buffer containing 1.5 M aminocaproic acid–2% (wt/vol) lauryl maltoside as described in reference 7. Blue native sample buffer was added as 1/10 of the final sample volume. For preparation of samples for SDS-PAGE analysis, the BN sample was diluted 1:1 with SDS sample buffer and was incubated for 30 min at room temperature. BN-PAGE and in-gel activity assays were performed with 5 to 15% BN-PAGE gels cast as described previously (7). After protein determination with the BCA kit (Pierce), gels were loaded with 30 μg protein per lane. Complex I and complex IV in-gel activity assays were performed with NADH–nitroblue tetrazolium and 3,3′-diaminobenzidine tetrahydrochloride, respectively, as described previously (7).

Cross-sectional area measurement. Images of sections stained with H&E were captured on a Leica microscope at a magnification of ×20. The cross-sectional area was quantified using ImageJ software.

Statistical analysis. Data were analyzed by one-way analysis of variance (ANOVA), followed by an appropriate *post hoc* test for comparison between two groups. Significance was defined as a P value of <0.05. Data are presented throughout as means ± standard deviations (SD) unless otherwise indicated.

Microarray data accession number. The microarray data determined in this study have been deposited in GEO under accession number GSE39009.

RESULTS

Specific skeletal muscle YY1 deficiency results in a dwarf-like mouse phenotype. Based on our previous findings in skeletal muscle cells that mitochondrial gene expression was affected by the transcription factor YY1 (10), we decided to generate skeletal-muscle-specific YY1 knockout (YY1mKO) mice to assess the biological function *in vivo*. YY1mKO mice had developmental growth and body weight similar to those of wild-type mice until approximately 2 months of age (Fig. 1A). At this point, whereas wild-type mice displayed a progressive normal growth curve, YY1mKO mice stopped growing and maintained a constant body weight, resulting in a dwarf-like phenotype (Fig. 1B). Interestingly, with age, YY1mKO mouse body weight started to decline, and mice exhibited signs of muscular dystrophy, such as curving of the back or kyphosis (Fig. 1C). MRI analysis showed that these differences in body weight did not result in any difference in the ratio between fat and lean mass (Fig. 1D). These changes in body weight occurred despite a significant increase in food intake in YY1mKO mice (see Fig. S1 in the supplemental material). These results indicate that specific expression of YY1 in skeletal muscle is required for whole-body postnatal growth and that its deficiency results in a dwarf-like mouse phenotype.

YY1mKO skeletal muscle exhibits abnormal mitochondrial morphology and distribution defects resembling mitochondrial myopathy. Because YY1 was specifically deleted in skeletal muscle, we visually inspected this tissue to determine whether any major abnormality existed. Figure 2A shows that the size of skeletal muscle tissue did not change significantly in young YY1mKO mice relative to that in wild-type mice, and at this resolution, they were apparently normal. It was noticed, however, that the color of the skeletal muscle was much paler in YY1mKO mice. This was particularly striking in the soleus muscle, which is characterized by a high mitochondrial content and oxidative capacity. Interestingly, this phenotype, which is suggestive of decreased mitochondrial mass, is similar to that of skeletal-muscle-specific raptor knockout (RamKO) mice (4) and opposite that of PGC1α transgenic mice (22). Next, we examined the skeletal muscles of YY1mKO mice by H&E staining. A deficiency of YY1 in the skeletal muscle resulted in high numbers of small fibers (Fig. 2B, black arrowheads), fibers with centralized nuclei (green arrowheads), and central core-like structures (blue arrowheads). Measurement

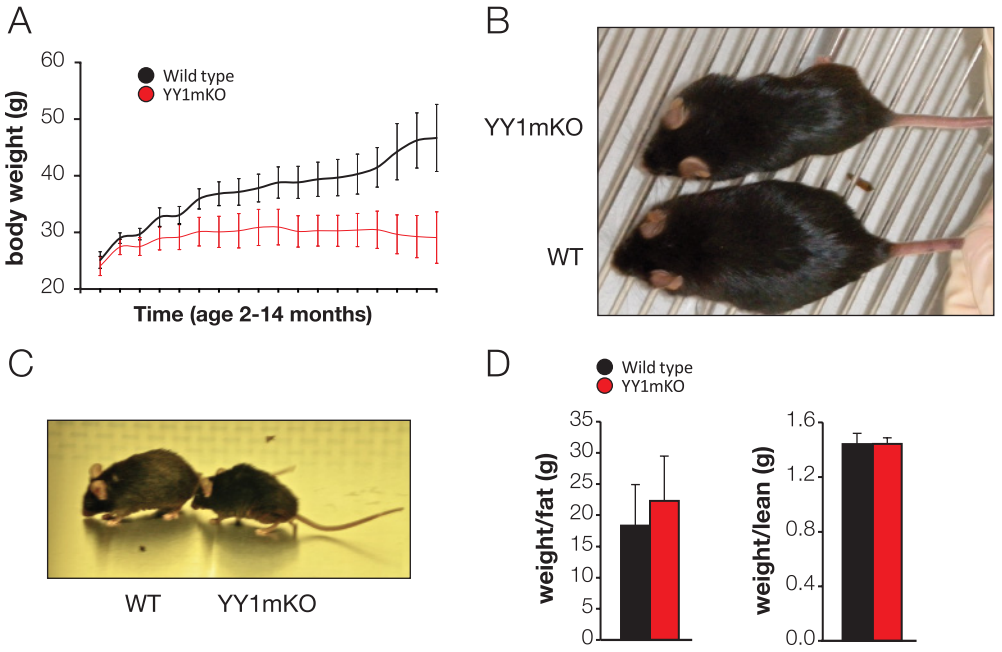

FIG 1 Specific genetic deletion of YY1 in skeletal muscle results in a dwarf phenotype. (A) The body weight of wild-type (WT) or YY1mKO mice (*n*, 9 to 10) was monitored for 1 year from the age of 2 months. (B) YY1mKO mice are smaller than wild-type mice (age, 1 year). (C) YY1mKO mice develop kyphosis (age, 1 year). (D) MRI of YY1mKO and wild-type mice (age, 1 year; $n = 10$).

of fiber cross-sectional areas in YY1mKO mice confirmed that these mice have a prevalence of small fibers compared to the normal fiber size distribution in wild-type mice (Fig. 2C). Moreover, 23% of fibers in these animals have centralized nuclei (Fig. 2D). To assess mitochondrial morphology, we performed electron microscopy (EM) of skeletal muscle from 6-month-old wild-type and YY1mKO mice (Fig. 3A). Electron micrographs from YY1mKO soleus muscle exhibited a very disorganized pattern of mitochondrial distribution along the different fibers (Fig. 3, compare panels a and b [wild type] with panels e and f [YY1mKO]). In addition, these organelles were more fragmented and contained defective and poorly formed cristae and intramitochondrial granules or vacuoles (Fig. 3A, compare panels c and d with panels g to k). This fragmentation might suggest impairments in the balance of mitochondrial processes such as fusion and fission. Furthermore, knockout mice show rod-like structures known as nemaline bodies, which are masses of anomalous Z-band material (Fig. 3Al). Consistent with the results from the H&E staining, YY1mKO muscle fibers have centralized nuclei (Fig. 3Aj), a sign of ongoing muscle regeneration. To determine if the mitochondrial defects observed in YY1mKO mice correlated with decreased mitochondrial function, we performed histochemistry on the gastrocnemius muscles of wild-type and knockout mice using staining assays for mitochondrial activity enzymes (Fig. 3B). The intensities of both succinate dehydrogenase (SDH) and cytochrome oxidase (COX) staining were decreased in knockout mice, suggesting decreased mitochondrial energetic activity. The glycogen content as measured by PAS staining, however, was not affected in YY1mKO mice. Taken together, these results indicate that YY1 deficiency in skeletal muscle causes significant aberrations in mitochondrial morphology and distribution as well as bioenergetic defects that might resemble some phenotypes associated with mitochondrial myopathies and diseases.

Mitochondrial genes encoding central bioenergetic metabolic pathways are downregulated in YY1mKO mouse skeletal muscle. Based on the facts that YY1 controls mitochondrial gene expression in cultured skeletal muscle cells (10) and that YY1mKO mice displayed strong derangements in mitochondria morphology, we performed genomewide expression profiling on total RNA isolated from wild-type and YY1mKO soleus muscles. Consistent with YY1 functioning as a repressor or activator of gene expression, we identified 978 genes whose expression was increased and 1,228 genes whose expression was decreased by use of a 1.5-fold change cutoff. Next, we performed GSEA to investigate if there was an enrichment for a pathway among the regulated genes in one or the other phenotype. In striking agreement with our previous work *in vitro* and the severe mitochondrial phenotype observed in the skeletal muscles of YY1mKO mice, among the 20 most significant gene sets enriched in the WT compared to the KO phenotype, 17 were associated with mitochondrial oxidative bioenergetic pathways, 2 were annotated as cancer subclasses—in which there was enrichment in mitochondrial genes—and 1 was a peroxisomal pathway (Fig. 4A). Based on our interest in the mitochondrial phenotype, we analyzed in more detail the mitochondrial pathways that were suppressed by YY1 deficiency in skeletal muscle. Among the mitochondrial pathways enriched, we found (i) oxidative phosphorylation (OXPHOS), (ii) energy metabolism, (iii) branched-chain amino acid catabolism, (iv) fatty acid oxidation, and (v) pyruvate metabolism and the tricarboxylic acid (TCA) cycle (Fig. 4B). In the "Mootha mitochondrial" gene set-enriched pathway, which contains a total of 370 genes, 166 genes displayed positive core enrichment (45%). In this list, additional genes were not clustered in the five mitochondrial pathways

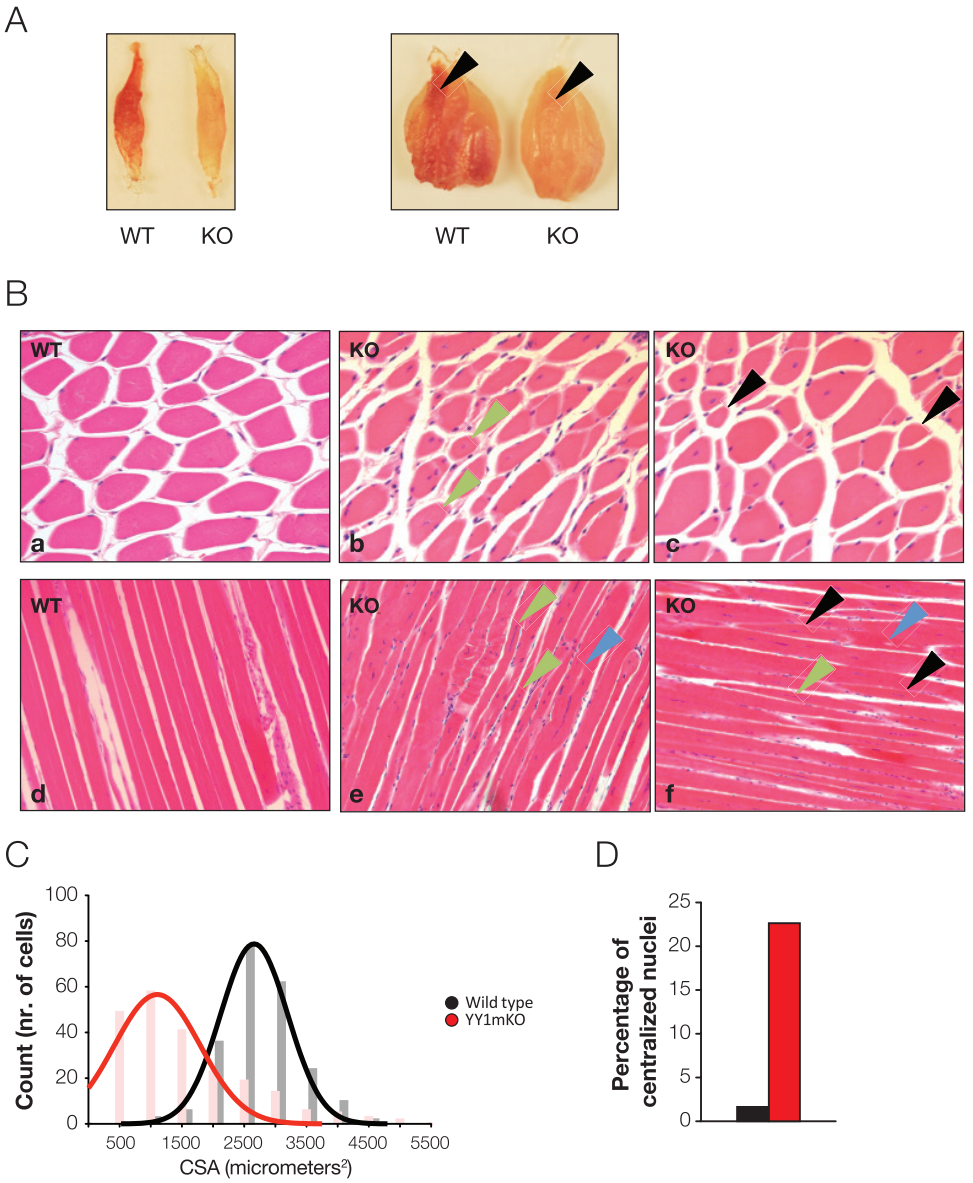

FIG 2 Deficiency of YY1 in skeletal muscle results in morphological mitochondrial defects. (A) Appearance of skeletal muscles of 3-month-old wild-type (WT) and YY1mKO mice. (Left) Soleus muscle; (right) the whole calf (gastrocnemius, soleus, and plantaris muscles). Arrowheads indicate the soleus. (B) (Top) Cross sections of gastrocnemius from 6-month-old male wild-type (a) or YY1mKO (b and c) mice stained with H&E. (Bottom) Longitudinal sections from wild-type (d) or YY1mKO (e and f) mice stained with H&E. Black arrowheads indicate small fibers; green arrowheads point to cells with centralized nuclei, and blue arrowheads point to central core-like structures. (C) Cross-sectional area (CSA) distribution in 6-month-old wild-type or YY1mKO fibers. (D) Percentages of cells with centralized nuclei in 6-month-old wild-type or YY1mKO fibers.

indicated. For example, mitochondrial ribosomal proteins, heme biosynthesis, reactive oxygen species (ROS) signaling, mitochondrial protein import, and mitochondrial fusion were downregulated in the skeletal muscles of YY1mKO mice. Of interest, one of the gene sets significantly downregulated in YY1mKO muscle was "Mootha_PGC," which contains 305 PGC1α muscle target genes and is enriched in mitochondrial genes (27). Of the 305 genes upregulated by PGC1α, 132 genes were downregulated in YY1mKO mice in this analysis. Importantly, specific gene changes measured in genomewide expression profiling were validated using quantitative real-time PCR. Figure 5A shows that the expression of genes clustered in the different mitochondrial pathways identified above was lower in YY1mKO mice than in wild-type mice. In addition, the expression of mitochondrial regulators, such as mitochondrial transcription factor A (mTFA), nuclear respiratory factors (NRFs), and estrogen-related receptor alpha (ERRα), but not proliferator-activated receptor gamma coactivator 1β (PGC1β) and peroxisome proliferator-activated receptor delta (PPARδ), was decreased in YY1mKO mice.

To determine whether YY1 directly regulated the mitochondrial bioenergetic genes, we analyzed the occupancy of this transcription factor at several of these gene promoters. As expected, based on predicted YY1 binding sites, YY1 was recruited at several

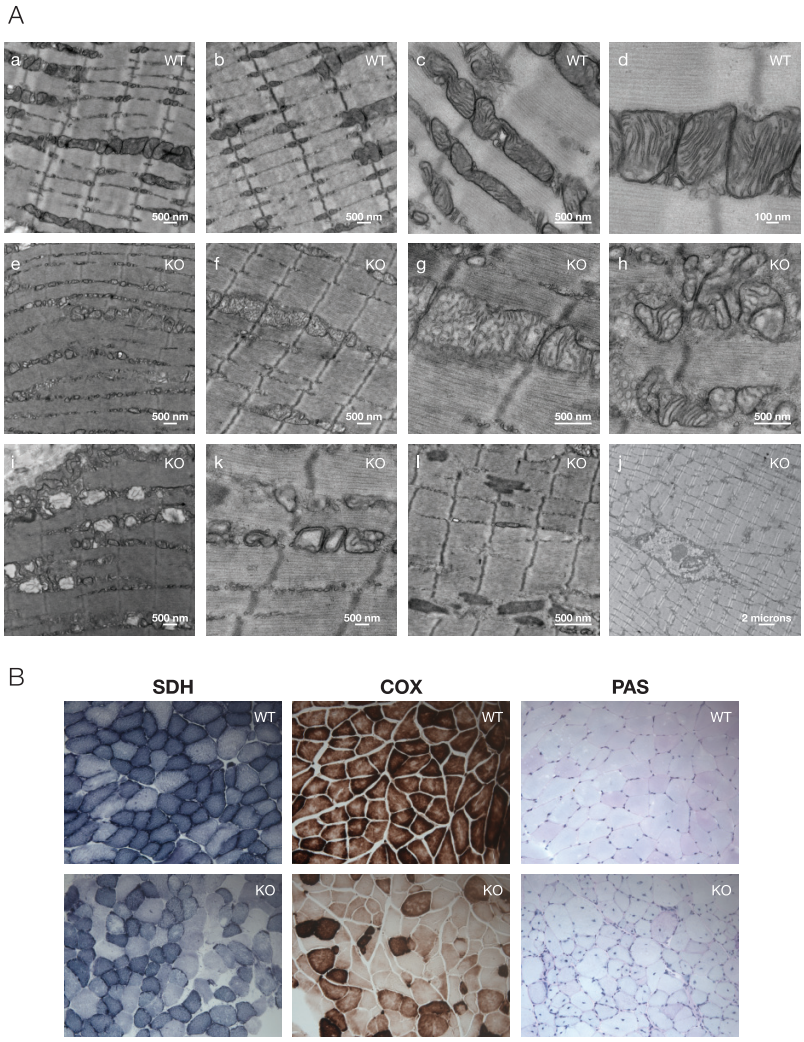

FIG 3 (A) Representative electron micrographs of soleus muscles of 6-month-old male wild-type (WT) (a to d) and YY1mKO (e to l) mice. (B) Histochemistry of mitochondrial proteins and glycogen. Succinate dehydrogenase (SDH) and cytochrome oxidase (COX) activities were determined, and glycogen staining with periodic acid-Schiff stain (PAS) was performed, on sections of gastrocnemius muscle from 6-month-old male mice.

proximal promoters of nuclear mitochondrial genes in skeletal muscle as well as in differentiated C_2C_{12} myotubes (Fig. 5B; see also Fig. S2A in the supplemental material). Taken together, these results indicate that YY1 is a positive and central regulator of a large number of mitochondrial genes involved in bioenergetic oxidative function.

YY1mKO skeletal muscle exhibits decreased expression of mitochondrial proteins and defective mitochondrial respiratory activity. To assess whether changes in mitochondrial gene expression observed in the skeletal muscles of YY1mKO mice translated into changes in protein levels, we analyzed protein extracts from gastrocnemius muscles of wild-type and YY1mKO mice. As shown in Fig. 6A, levels of mitochondrial proteins from the different respiratory chain complexes were decreased in YY1mKO skeletal muscle. In particular, proteins in complex I (Nduf9a and Ndufs3) and in complex IV (Cox5a) were strongly downregulated in YY1mKO mice. Next, to assess whether these decreases in mitochondrial proteins resulted in functional defects in complex activity, we measured the in-gel activities of mitochondrial complexes I and IV. Consistent with diminished protein subunit levels, the activities of complex I and IV were significantly decreased in YY1mKO skeletal muscle (Fig. 6B). To further determine mitochondrial bioenergetic dysfunction in the skeletal muscles of YY1mKO mice, we isolated mitochondria from gastrocnemius muscles and performed oxygen consumption measurements using a Seahorse XF analyzer. Mitochondrial pellet preparations from YY1mKO muscles were smaller and paler, suggesting a reduction of the levels of mitochondrial cytochromes (data not shown). The bioenergetic profile of YY1mKO mitochondria showed decreased complex I-driven oxygen consumption rates in all respiratory states (ranging from a 42% to a 73% decrease relative to the same amount of mitochondrial protein from wild-type mice), indicating overall decreased electron transport chain activity (Fig. 6C). Collectively, these data indicate that YY1 deficiency in skeletal muscle strongly compromises mitochondrial bioenergetic capacity.

YY1 deficiency in skeletal muscle causes exercise intolerance. Defects in mitochondrial oxidative function in skeletal muscle are

A

NAME	SIZE	ES	NES	NOM p-val	FDR q-val	FWER p-val
KEGG_VALINE_LEUCINE_AND_ISOLEUCINE_DEGRADATION	41	-0.8500	-2.5273	0	0	0
KEGG_FATTY_ACID_METABOLISM	34	-0.8457	-2.4454	0	0	0
WONG_MITOCHONDRIA_GENE_MODULE	183	-0.6299	-2.4144	0	0	0
KEGG_PEROXISOME	63	-0.7239	-2.3790	0	0	0
MOOTHA_FFA_OXIDATION	19	-0.9176	-2.3603	0	0	0
MOOTHA_HUMAN_MITODB_6_2002	365	-0.5799	-2.3537	0	0	0
KEGG_PROPANOATE_METABOLISM	28	-0.8431	-2.3415	0	0	0
REACTOME_GLUCOSE_REGULATION_OF_INSULIN_SECRETION	132	-0.6400	-2.3347	0	0	0
REACTOME_ELECTRON_TRANSPORT_CHAIN	59	-0.7213	-2.3201	0	0	0
KEGG_PPAR_SIGNALING_PATHWAY	59	-0.7083	-2.2966	0	0	0
MOOTHA_MITOCHONDRIA	370	-0.5586	-2.2801	0	0	0
KEGG_CITRATE_CYCLE_TCA_CYCLE	27	-0.8143	-2.2571	0	0	0
MOOTHA_VOXPHOS	75	-0.6660	-2.2361	0	0	0
REACTOME_CITRIC_ACID_CYCLE	18	-0.8907	-2.2225	0	0	0
REACTOME_INTEGRATION_OF_ENERGY_METABOLISM	184	-0.5786	-2.2183	0	0	0
STEIN_ESRRA_TARGETS_UP	270	-0.5599	-2.2179	0	0	0
REACTOME_PYRUVATE_METABOLISM_AND_TCA_CYCLE	31	-0.7749	-2.2165	0	0	0
CHIANG_LIVER_CANCER_SUBCLASS_PROLIFERATION_DN	112	-0.6048	-2.1919	0	0	0
REACTOME_REGULATION_OF_INSULIN_SECRETION	173	-0.5712	-2.1566	0	0	0
BOYAULT_LIVER_CANCER_SUBCLASS_G123_DN	41	-0.7239	-2.1462	0	2.93E-05	0.001

B

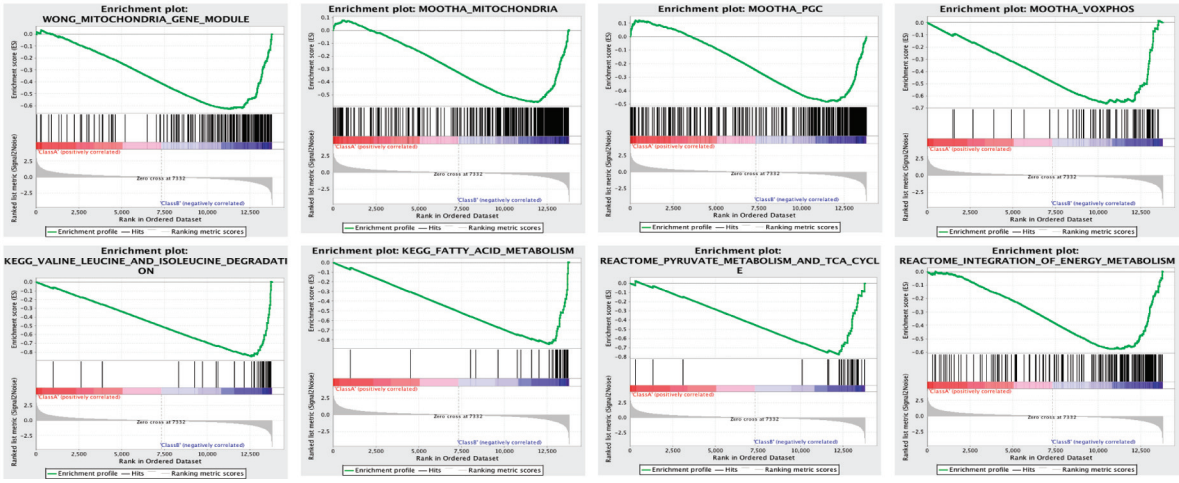

FIG 4 Mitochondrial metabolic genes are downregulated in YY1mKO skeletal muscle. (A) GSEA of the top 20 pathways downregulated in soleus muscles of 3-month-old YY1mKO mice. Red represents mitochondrial pathways, green represents cancer-related pathways, and blue represents the peroxisomal pathway. ES, enrichment score; NES, normalized enrichment score; NOM p-val, nominal *P* value; FDR q-val, probability for false discovery rate; FWER p-val, familywise error rate. (B) Enrichment plots for representative gene expression sets. The color bar depicts the gene list used in the GSEA ordered by differential gene expression. Red indicates higher (positively correlated) and blue indicates lower(negatively correlated) signal to noise in WT compared to YY1mKO mice.

a clinical symptom of mitochondrial myopathies and cause important difficulties for physical exercise (38, 40, 51). Given that YY1mKO mice displayed severe mitochondrial abnormalities and bioenergetic deficits in skeletal muscle, we investigated whether the ability to perform exercise was altered in these mice. Three different types of exercise tests were performed with wild-type and YY1mKO mice. In the forced treadmill performance to exhaustion, YY1mKO mice ran an average of 59 min and 1,077.5 m, compared to 90 min and 1,721.5 m for wild-type mice (Fig. 7A and B). Moreover, wild-type mice scored a mean of 2.5 falls from the treadmill in 10 min, whereas YY1mKO mice scored 12.5 (Fig. 7C). In the voluntary wheel performance, wild-type mice spent approximately 4 times more time in the wheel than did YY1mKO mice (Fig. 7D). These experiments suggest that consistent with the defects in mitochondrial function observed in YY1mKO mice, these mice are intolerant to exercise, a signature often manifested in mitochondrial diseases.

Mitochondrial genes are not suppressed by rapamycin in YY1mKO mice. We have reported previously that rapamycin suppresses mitochondrial genes in cultured cells and in skeletal muscle in mice (5, 10). It was not clear, however, whether this suppression required YY1 *in vivo*. To address this, we treated wild-type and YY1mKO mice with rapamycin for 2 weeks and analyzed gene expression in skeletal muscle. As expected, levels of transcripts, including those of transcriptional regulatory genes, OXPHOS genes, and fatty acid oxidation genes, were decreased upon rapamycin treatment in wild-type mice (Fig. 8A). All the genes in this list were downregulated in YY1mKO mice, but importantly, rapamycin did not further decrease the expression of these genes. Moreover, these effects were cell autonomous, since YY1-depleted myotubes that were treated with rapamycin followed the same gene expression pattern (Fig. 8B). In addition, the protein levels of some of these mitochondrial genes were also reduced by rapamycin in myotubes (see Fig. S2B in the supplemental material). To test whether the effects of rapamycin occurred through mTORC1, we used skeletal-muscle-specific raptor knockout mice (4). Consistent with previous reports, RamKO mice exhibited decreased mitochondrial gene expression and, like YY1mKO mice, were in-

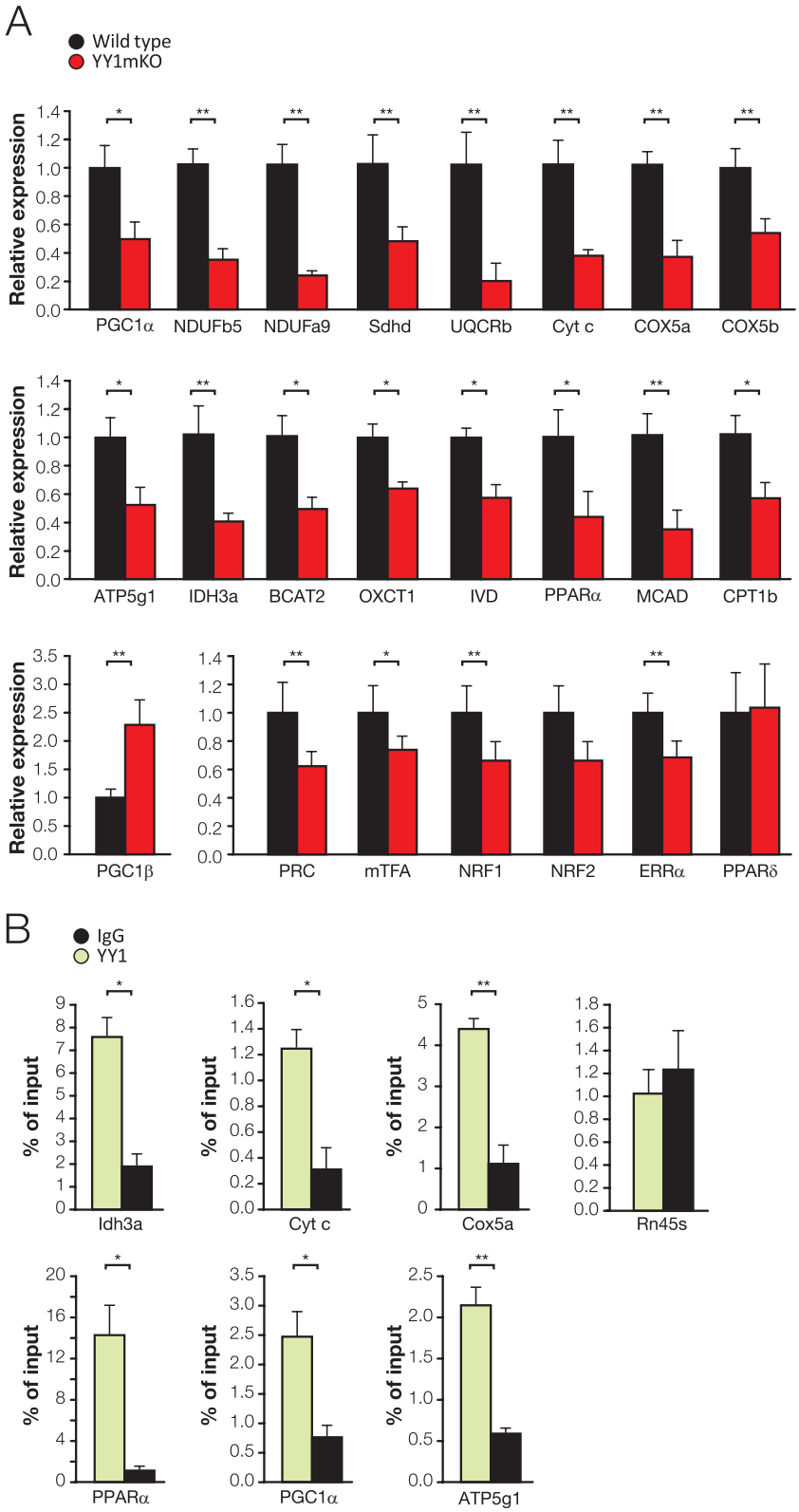

FIG 5 Deficiency of YY1 in skeletal muscle results in decreases in the expression of mitochondrial and transcriptional regulatory mitochondrial genes. (A) Gene expression was measured by quantitative real-time PCR from soleus muscle RNA extracted from 3 month-old fed mice. (B) ChIP analysis from gastrocnemius muscles of 3 month-old fed mice. All values are presented as means ± SD. Four to 10 mice were used. *, $P < 0.05$; **, $P < 0.01$.

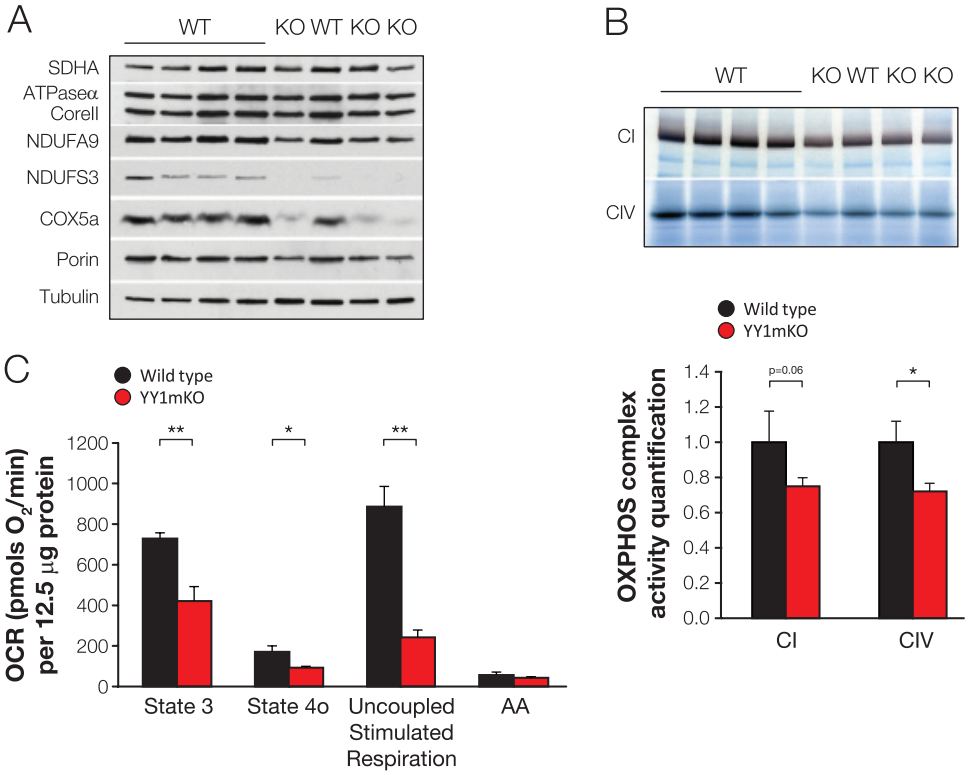

FIG 6 YY1mKO skeletal muscles have lower expression of mitochondrial proteins and lower levels of mitochondrial electron chain respiratory activity. (A) Western blots of mitochondrial proteins in skeletal muscle. (B) OXPHOS complex activities measured by in gel-activity assays (top) and relative quantification (bottom). (C) Oxygen consumption rates (OCR) measured from total mitochondrial fractions isolated from wild-type and YY1mKO gastrocnemius muscles. Bars show average OCR values from 4 to 5 mice per group ± standard errors of the means. The substrates used were 5 mM pyruvate plus 5 mM malate. State 3 (OCR associated with maximal ATP synthesis rates) was induced with 1 mM ADP. State 4o (proton leak, respiration independent of ATP synthesis) was induced by 2 μM oligomycin (complex V inhibitor). Electron transport chain activity independent of ATP synthesis (uncoupled) was induced by 4 μM FCCP. Nonmitochondrial electron transport OCR (background) were determined by the addition of the complex III inhibitor antimycin A (AA). Asterisks indicate significant differences (*, $P < 0.05$; **, $P < 0.01$) by an unpaired, two-tailed Student *t* test.

sensitive to the suppressive effects of rapamycin on these genes. Interestingly, the YY1 mRNA levels were also decreased in these mice (Fig. 8C). These data indicate that the downregulated mitochondrial gene expression caused by mTORC1 inactivation (either pharmacologically or genetically) requires the transcription factor YY1.

mTORC1-dependent phosphorylation of YY1 recruits PGC1α and increases mitochondrial gene expression and bioenergetic function. We next investigated the mechanisms by which mTORC1 inactivation mediates the suppression of mitochondrial genes through YY1. We have previously determined that the interaction between YY1 and PGC1α is disrupted upon rapamycin treatment (10). In addition, we recently showed that two YY1 sites (T30 and S365) are phosphorylated only when mTORC1 is active (5). To address whether these specific YY1 phosphorylation sites regulate the mTORC1-dependent interaction with PGC1α, we performed immunoprecipitation analysis using a YY1 mutant allele (YY1-AA) that prevents phosphorylation (T30A S365A) in C_2C_{12} myotubes and HEK-293 cells. As predicted, wild-type YY1 interacted with PGC1α, and rapamycin decreased the strength of this interaction (Fig. 9A and B). Consistent with the data showing that mTOR-dependent phosphorylation of these two residues maintains the interaction between YY1 and PGC1α, the YY1-AA mutant had very weak binding to PGC1α and was insensitive to rapamycin.

In order to support the notion that mTOR controlled YY1 through phosphorylation at the sites identified, we assessed the functionality of YY1 alleles in transcriptionally based luciferase assays using the cytochrome *c* promoter, which contains binding sites for YY1. Figure 9C shows that wild-type YY1 increased the transcriptional activity of the cytochrome *c* promoter, which was further enhanced with PGC1α expression. These YY1-dependent transcriptional activities were suppressed by rapamycin. YY1-AA had a mild repressing effect on the basal activity of the cytochrome *c* promoter; nevertheless, the overexpression of YY1-AA blunted the effects of YY1 and PGC1α activation, consistent with the possibility that this mutant acts as a dominant negative mutant. In line with the physical interactions, the effect of YY1-AA was insensitive to rapamycin treatment.

Next, we evaluated these transcriptional effects on endogenous YY1 and PGC1α target genes using adenoviral infection in differentiated primary skeletal muscle cells. Figure 9D shows that wild-type YY1 increases the expression of a broad range of mitochondrial genes; of note, the expression of other transcriptional regulators of these genes, including PGC1α and PPARα, was strongly elevated by YY1. In agreement with the data on interaction with PGC1α, overexpression of YY1-AA did not result in increases in the expression of these genes; in fact, it further downregulated basal gene expression, suggesting again that it might act as a dominant negative mutant on endogenous YY1. These regu-

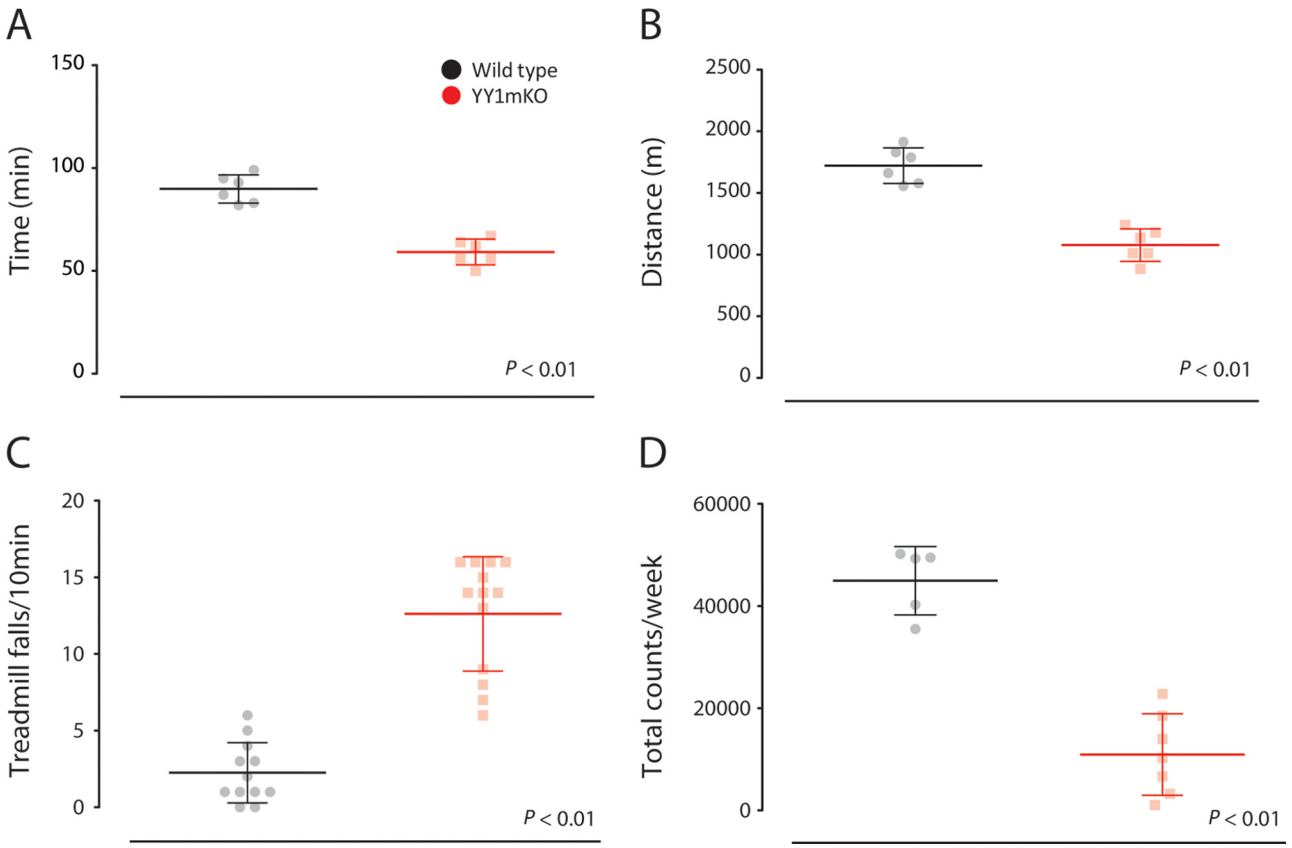

FIG 7 YY1mKO mice exhibit exercise intolerance. (A and B) Six-month-old male wild-type and YY1mKO mice were subjected to forced treadmill performance until exhaustion, and time (A) and distance (B) were recorded. (C) Number of stops/falls from the treadmill. (D) Voluntary wheel performance. Five to 13 mice were tested. *, $P < 0.01$.

latory effects of YY1 alleles were consistent with the recruitment of wild-type YY1, but not YY1-AA, to the promoter regions of several mitochondrial genes (Fig. 10A). Importantly, all these changes in physical interactions and in gene expression translated into changes in mitochondrial bioenergetic activities. We again used the Seahorse technology to assess oxygen consumption in myotubes infected with the different YY1 alleles. Expression of wild-type YY1, but not YY1-AA, increased oxygen consumption rates (Fig. 10B). In fact, both basal respiration and maximal respiratory capacity were higher than those for the control with wild-type YY1 but lower with YY1-AA. Taken together, these results indicate that mTOR-mediated phosphorylation on YY1 directly controls the expression of mitochondrial regulatory genes and bioenergetic function.

Finally, based on the robust activation of mitochondrial genes by PGC1α in skeletal muscle cells, we sought to test the requirement of YY1 for PGC1α coactivation of shared target genes. Figure 10C shows that increases in the expression of PGC1α target mitochondrial genes were substantially attenuated in myotubes depleted of YY1 by shRNA, suggesting that YY1 is required for PGC1α to produce full activation of mitochondrial genes.

DISCUSSION

In this study, we have unraveled the physiological role of YY1 in skeletal muscle, which is to maintain normal mitochondrial function and morphology. A deficiency of YY1 in this tissue causes strong suppression of a large number of mitochondrial genes, leading to severe mitochondrial abnormalities. YY1 recruits the transcriptional coactivator PGC1α to increase mitochondrial gene expression. This recruitment requires mTOR activity-dependent YY1 phosphorylation, which promotes the interaction between YY1 and PGC1α. Overall, these results support a pivotal function of YY1 in maintaining mitochondrial structure and function and provide the molecular basis of how YY1 inactivation results in a phenotype resembling mitochondrial myopathies.

The transcription factor YY1 can function as an activator or repressor of gene transcription involved in different cellular processes, but the specific mechanisms underlying this dual function are unclear (6, 15, 24, 39). In repression, YY1 is associated with histone deacetylase (HDAC) corepressor complexes, but the selective recruitment to promoters has not been elucidated (42, 50). In *Drosophila*, the YY1 homolog called Pleiohomeotic is a Polycomb protein found in complexes involved in gene repression and silencing (2, 45). Of several Polycomb proteins in mammals, only Pc2 (part of the PRC1 complex) (17) associates with YY1 under conditions of mTOR inactivation, and this interaction depends on the two mTOR-dependent phosphorylation sites T30 and S365 (5). When YY1 functions as an activator, it recruits coactivators such as p300 and INO80 (3, 6), but how they selectively bind to promoters to activate YY1 transcriptional function is unknown. Within the context of mitochondrial gene expression, we show here that YY1 activation is assigned to recruitment of the PGC1α

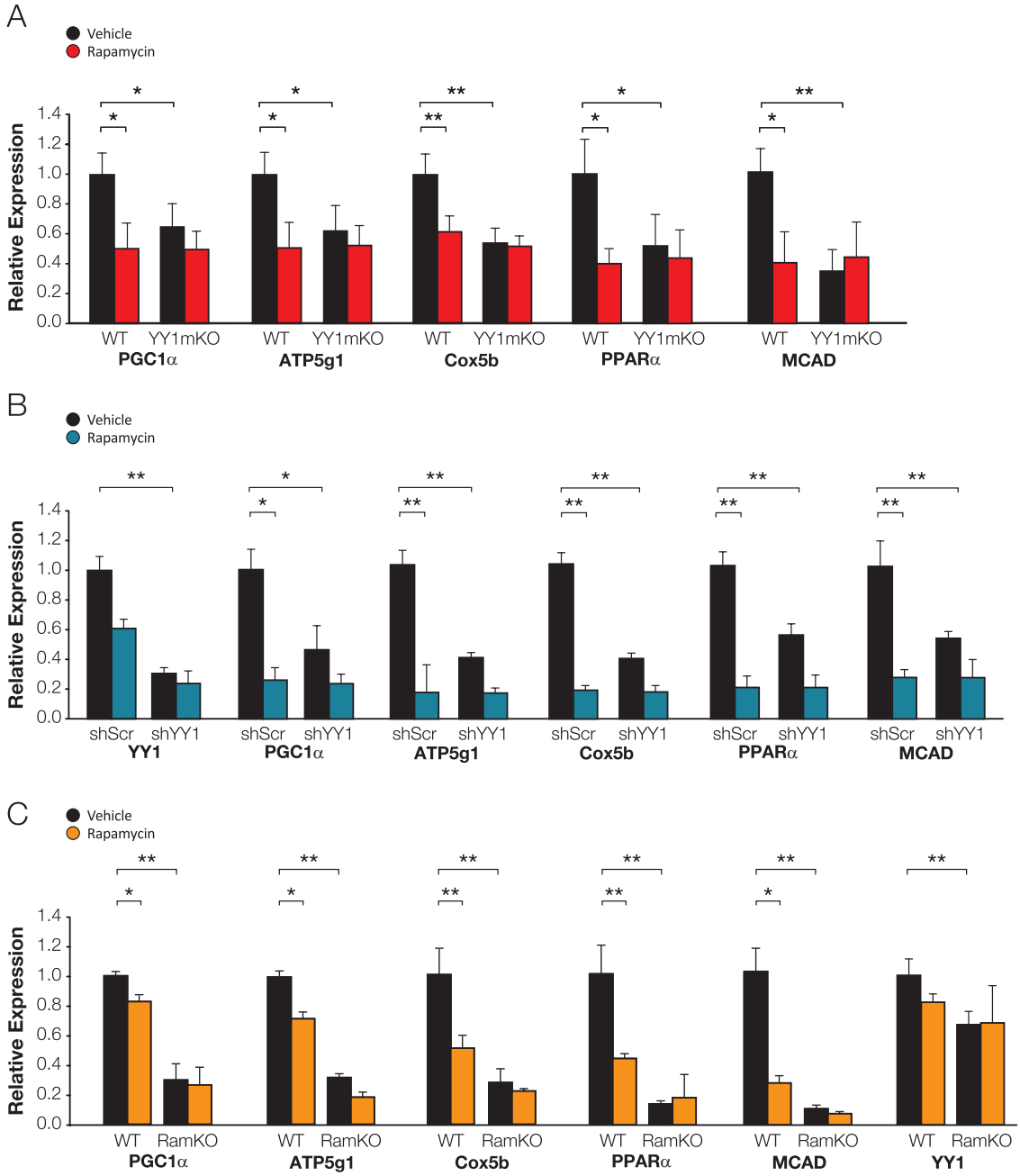

FIG 8 Rapamycin does not suppress mitochondrial genes in YY1mKO or RamKO mice. (A) Six-month-old male wild-type and YY1mKO mice were treated with a vehicle or 2.5 mg/kg rapamycin for 14 days. Gene expression was measured by quantitative real-time PCR from soleus RNA extracted from fed mice. (B) C_2C_{12} myotubes were infected with control scrambled shRNA (shScr) or shYY1 for 48 h, and gene expression was measured by quantitative real-time PCR. (C) Three-month-old male wild-type or RamKO mice were treated with a vehicle or 2.5 mg/kg rapamycin for 14 days. Gene expression was measured by quantitative real-time PCR from soleus RNA extracted from fed mice. All values are presented as means ± SD. Four to 10 mice were used. *, $P < 0.05$; **, $P < 0.01$.

transcriptional coactivator, which, in contrast to Pc2, is recruited to YY1 when mTOR is active. Therefore, these data might explain, at least in part, promoter-specific YY1 activation or repression function.

Taken together, the data we present here and our recent data showing that YY1 controls insulin/insulin growth factor (IGF) signaling genes (5) indicate that YY1 regulates two major metabolic pathways: insulin/IGF signaling and mitochondrial function. It is interesting, however, that despite impaired mitochondrial oxidative function, hyperactivation of insulin/IGF signaling in YY1mKO mice is sufficient to increase insulin sensitivity. In fact, contrary to the prediction that mitochondrial defects would exacerbate insulin resistance, YY1mKO mice are insulin sensitive due to increases in insulin/IGF signaling, suggesting that hyperactivation of this pathway can override the mitochondrial dysfunction in these mice.

YY1 forms part of a group of transcription factors that control many mitochondrial genes, as illustrated by the gene set enrich-

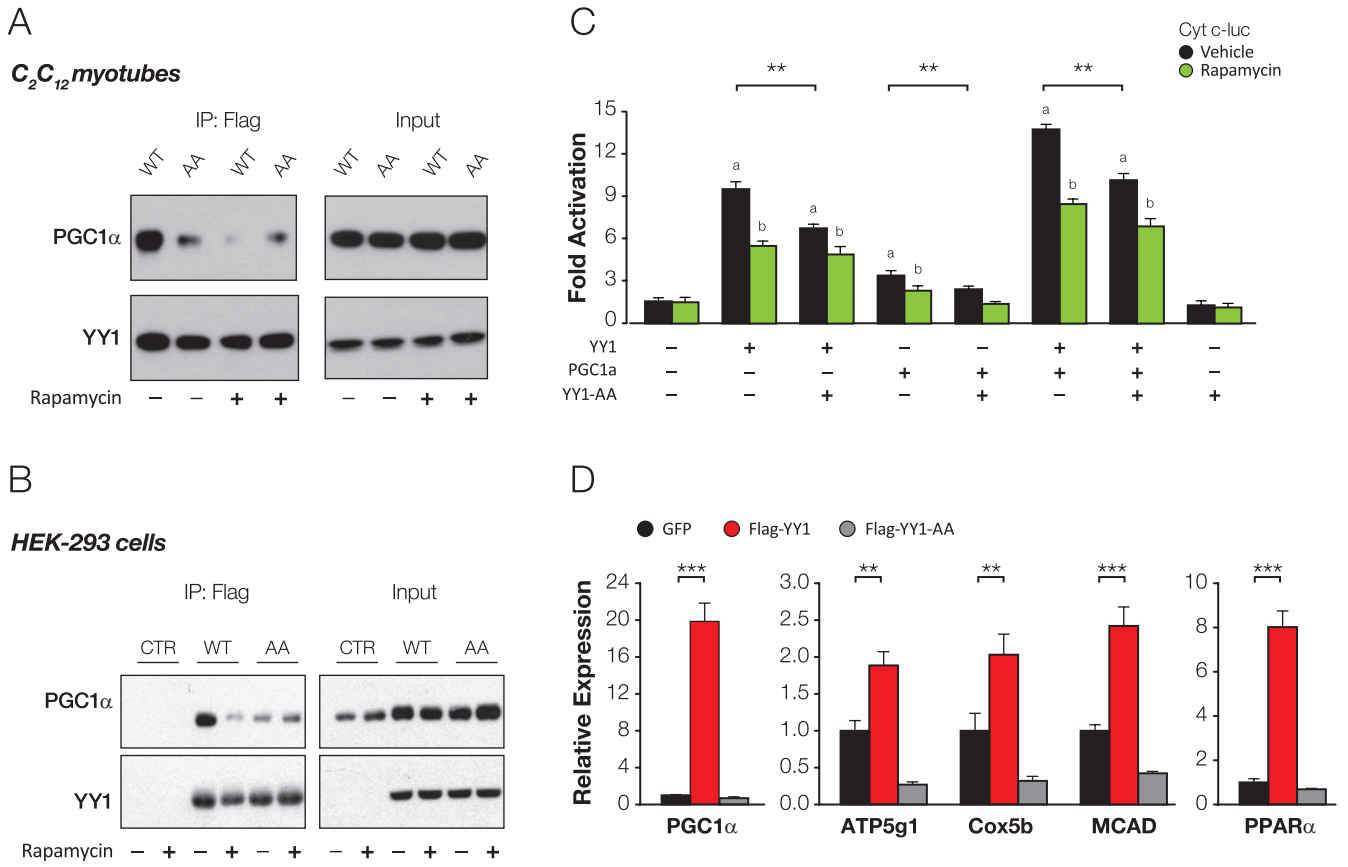

FIG 9 mTORC1-dependent phosphorylation of YY1 recruits PGC1α and increases mitochondrial gene expression and bioenergetic function. (A) Coimmunoprecipitation of Flag-labeled YY1 and hemagglutinin (HA)-labeled PGC1α in C_2C_{12} myotubes treated with a vehicle or 20 nM rapamycin for 2 h. IP, immunoprecipitation. (B) Coimmunoprecipitation of Flag-YY1 and HA-PGC1α in HEK-293 cells treated with a vehicle or 20 nM rapamycin for 2 h. (C) Luciferase assay in HEK-293 cells transfected with a cytochrome *c* luciferase construct and the indicated proteins. Rapamycin (20 nM) was added as indicated 24 h before cell lysis. Data are expressed as fold activation and were normalized to the level of expression in an empty-vector-transfected control. a, significant difference ($P < 0.01$) between the control and the overexpressed plasmid; b, significant difference ($P < 0.01$) between the vehicle and rapamycin; **, $P < 0.01$. (D) Primary muscle myotubes were infected with green fluorescent protein (GFP), Flag-YY1, or Flag-YY1-AA for 48 h, and gene expression was measured by quantitative real-time PCR. All values are presented as means ± SD. Four to 10 mice were used. **, $P < 0.01$; ***, $P < 0.001$.

ment analysis performed in these studies. Thus, nuclear YY1 maintains the activation of mitochondrial genes encoding proteins involved in different mitochondrial processes, from bioenergetics to protein import, that are necessary for the formation of proper structural and functional organelles. Indeed, YY1 binding sites are present in a large number of mitochondrial genes where YY1 is recruited (Fig. 5B) (13), and part of this activation is due to PGC1α, which is both induced and coactivated by YY1. Nevertheless, in our microarray analysis, we identified some mitochondrial respiratory genes that are not regulated by YY1 (see Fig. S3 in the supplemental material), suggesting a specific rather than a general regulation of this pathway. The global effects of YY1 on mitochondrial gene expression are part of a complex transcriptional network with synergies among the different components. This is exemplified by the interaction presented here between YY1 and PGC1α, which would impact additional transcription factors, such as NRFs and ERRs, that control mitochondrial gene expression and are coactivated by PGC1α (18, 26, 36, 48). An important question is under what regulatory conditions YY1 operates to increase mitochondrial gene expression. Our results indicate that in the context of mTOR activation, YY1 remained bound to the transcriptional coactivator PGC1α and that these genes were activated. It is conceivable, however, that other regulatory pathways impinge on YY1 without changes in mTOR activity. For example, increases in PGC1α levels that occur through activation of different signaling pathways involving cyclic AMP (cAMP) or calcium signaling (30, 47) could allow more binding between YY1 and PGC1α. Alternatively, although mTOR activity controls YY1 T30 and S365 phosphorylation, other, additional kinases and/or phosphatases could regulate the phosphorylation of these residues on YY1 independently of mTOR.

At this point, it is not clear how much of the effect of PGC1α on mitochondrial genes is mediated by YY1. In an attempt to answer this question, we measured the effect of PGC1α on mitochondrial genes in C_2C_{12} myotubes that were depleted of YY1 by shRNA (Fig. 10C). YY1 reduction decreased the effects of PGC1α 2-fold. It is difficult to interpret these data, because YY1 is depleted only to 50% by shRNA. However, it is likely that other transcription factors, including NRFs and ERRα, could work independently of YY1 and thus explain the residual PGC1α effects on mitochondrial genes in YY1 shRNA cells.

A deficiency of YY1 in skeletal muscle causes impaired postna-

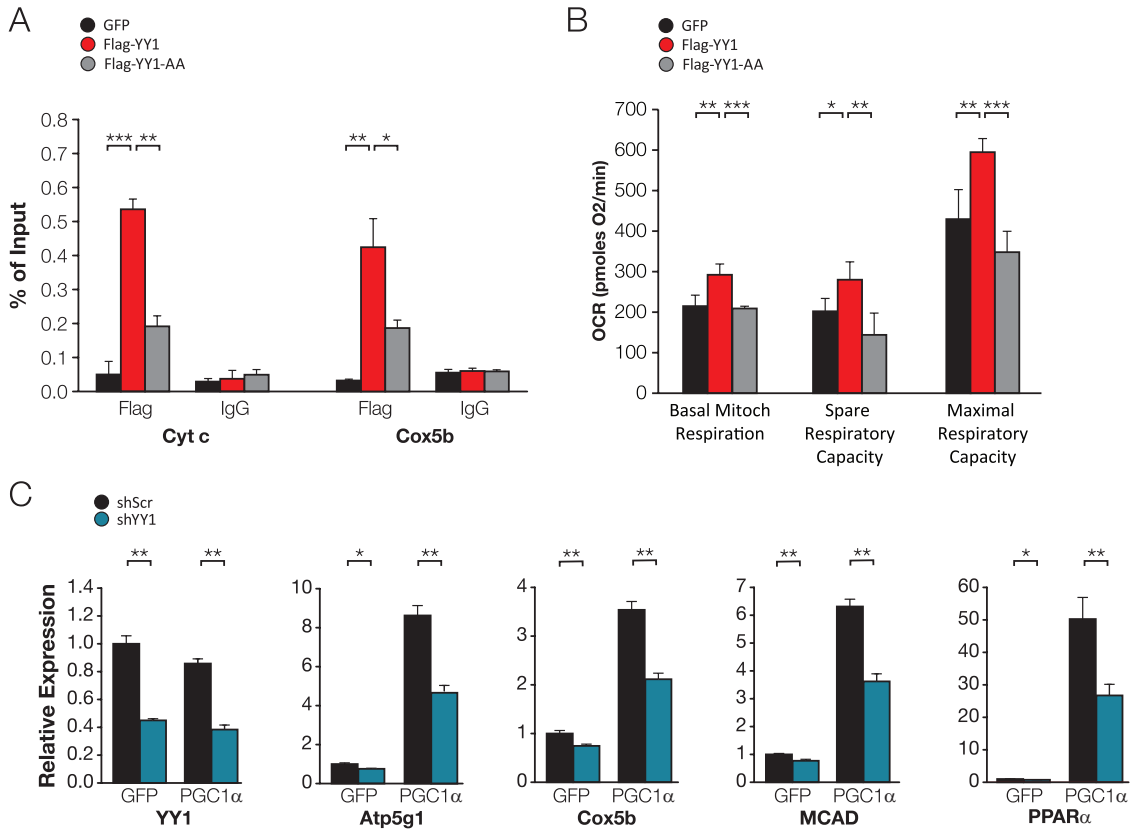

FIG 10 YY1 binds to nuclear mitochondrial genes and increases oxygen consumption in cultured muscle cells. (A) ChIP was performed in C_2C_{12} myotubes using antibodies specific for Flag or IgG. All values are presented as means ± standard errors of the means. Four mice were used. *, $P < 0.05$; **, $P < 0.01$; ***, $P < 0.001$. Cyt c, cytochrome *c*. (B) Oxygen consumption rates (OCR) in C_2C_{12} myotubes infected with green fluorescent protein (GFP), Flag-YY1, or Flag-YY1-AA. Mitoch, mitochondrial. (C) C_2C_{12} myotubes were infected with either shScrambled or shYY1 and with GFP or PGC1α for 72 h, and gene expression was measured by quantitative real-time PCR. All values are presented as means ± SD. Four to 10 mice were used. *, $P < 0.05$; **, $P < 0.01$.

tal growth and a dwarf phenotype. The mechanisms by which YY1 in this tissue is necessary to promote normal growth are unknown, but the findings suggest that YY1 might control the action of systemic factors, such as growth hormone, necessary for whole-body growth. Of interest, in some types of mitochondrial myopathies, patients often present a short stature, suggesting that mitochondrial dysregulation in skeletal muscle might be an underlying cause of defective postnatal growth (46). Nevertheless, since YY1 also controls genes involved in the cell cycle and translation, we could not exclude the possibility that the defective growth is due to a decrease in these pathways. However, our results show that cell cycle genes and protein translation are increased in YY1mKO mice (see Fig. S4 in the supplemental material).

In agreement with mitochondrial dysfunction, a deficiency of YY1 in skeletal muscle causes exercise intolerance. The positive regulatory roles of PGC1α and mTORC1 in exercise are well established (4, 22), and we show here that YY1, which interacts with mTORC1 and PGC1α (Fig. 9A and B) (10), is also necessary to maintain full exercise capabilities. Exercise intolerance in YY1mKO mice is also consistent with the profound mitochondrial defects observed in different genetic models of mTOR and PGC1α in skeletal muscle (4, 22, 32). In this sense, regulation of mTOR during exercise might maintain mitochondrial function through YY1/PGC1α transcriptional activity. It is also conceivable that loss of YY1 in skeletal muscle affects other components of the muscle fiber involved in contraction and movement. For example, we observed that several genes associated with skeletal muscle dystrophy are affected in YY1mKO mice, and at older ages, these mice developed kyphosis. These signs of dystrophy, however, are not as severe as those described in skeletal-muscle-specific mTOR or raptor KO mice (4, 32).

In addition, YY1 deficiency resembles several models of mitochondrial myopathies and diseases, a finding mechanistically supported by the direct transcriptional control of YY1 at the promoters of a large number of mitochondrial genes, some of them mutated in these diseases. Nevertheless, at present we cannot exclude the possibility that other pathways besides mitochondria contribute to the exercise phenotype in YY1mKO mice.

In summary, our studies reveal a key role of the transcription factor YY1 in maintaining the expression of a large number of mitochondrial genes in skeletal muscle that are responsible for retaining mitochondrial structure and function. A deficiency of YY1 in skeletal muscle results in reduced exercise capability and the appearance of signs of mitochondrial myopathy. Finally, these results would predict the possibility that increases in YY1 activity, like increases in mTORC1 and PGC1α activities, might improve skeletal muscle function and help to prevent several types of mitochondrial myopathies.

ACKNOWLEDGMENTS

We thank the members of the Puigserver lab for advice and fruitful discussions, Christine Chin for technical assistance, Eric Olson for the myogenin CRE mice, and Sebastian Valentin, Roderick Bronson, and Maria Ericsson for help with histochemistry, H&E staining, and electron microscopy, respectively. We also thank James White for advice on exercise protocols and cross-sectional area measurements.

These studies were supported by a postdoctoral fellowship from the Swiss National Science Foundation (to S.M.B.) and by NIH/NIDDK grant RO1 DK081418 and Muscular Dystrophy Association grant MDA202237 (to P.P.).

REFERENCES

1. **Affar EB, et al.** 2006. Essential dosage-dependent functions of the transcription factor yin yang 1 in late embryonic development and cell cycle progression. Mol. Cell. Biol. **26**:3565–3581.
2. **Atchison L, Ghias A, Wilkinson F, Bonini N, Atchison ML.** 2003. Transcription factor YY1 functions as a PcG protein in vivo. EMBO J. **22**:1347–1358.
3. **Austen M, Luscher B, Luscher-Firzlaff JM.** 1997. Characterization of the transcriptional regulator YY1. The bipartite transactivation domain is independent of interaction with the TATA box-binding protein, transcription factor IIB, TAFII55, or cAMP-responsive element-binding protein (CPB)-binding protein. J. Biol. Chem. **272**:1709–1717.
4. **Bentzinger CF, et al.** 2008. Skeletal muscle-specific ablation of raptor, but not of rictor, causes metabolic changes and results in muscle dystrophy. Cell Metab. **8**:411–424.
5. **Blättler SM, et al.** 2012. Yin Yang 1 deficiency in skeletal muscle protects against rapamycin-induced diabetic-like symptoms through activation of insulin/IGF signaling. Cell Metab. **15**:505–517.
6. **Cai Y, et al.** 2007. YY1 functions with INO80 to activate transcription. Nat. Struct. Mol. Biol. **14**:872–874.
7. **Calvaruso MA, Smeitink J, Nijtmans L.** 2008. Electrophoresis techniques to investigate defects in oxidative phosphorylation. Methods **46**:281–287.
8. **Calvo SE, Mootha VK.** 2010. The mitochondrial proteome and human disease. Annu. Rev. Genomics Hum. Genet. **11**:25–44.
9. **Canto C, Auwerx J.** 2010. AMP-activated protein kinase and its downstream transcriptional pathways. Cell. Mol. Life Sci. **67**:3407–3423.

9a. **Chappell JB, Perry SV.** 1954. Biochemical and osmotic properties of skeletal muscle mitochondria. Nature **173**:1094–1095.

10. **Cunningham JT, et al.** 2007. mTOR controls mitochondrial oxidative function through a YY1-PGC-1α transcriptional complex. Nature **450**:736–740.
11. **Eichner LJ, Giguere V.** 2011. Estrogen related receptors (ERRs): a new dawn in transcriptional control of mitochondrial gene networks. Mitochondrion **11**:544–552.
12. **Finck BN, Kelly DP.** 2006. PGC-1 coactivators: inducible regulators of energy metabolism in health and disease. J. Clin. Invest. **116**:615–622.
13. **Goffart S, Wiesner RJ.** 2003. Regulation and co-ordination of nuclear gene expression during mitochondrial biogenesis. Exp. Physiol. **88**:33–40.
14. **Handschin, C, Spiegelman BM.** 2011. PGC-1 coactivators and the regulation of skeletal muscle fiber-type determination. Cell Metab. **13**:351–352.
15. **He Y, et al.** 2007. The transcription factor Yin Yang 1 is essential for oligodendrocyte progenitor differentiation. Neuron **55**:217–230.
16. **Hock MB, Kralli A.** 2009. Transcriptional control of mitochondrial biogenesis and function. Annu. Rev. Physiol. **71**:177–203.
17. **Kagey MH, Melhuish TA, Wotton D.** 2003. The polycomb protein Pc2 is a SUMO E3. Cell **113**:127–137.
18. **Kelly DP, Scarpulla RC.** 2004. Transcriptional regulatory circuits controlling mitochondrial biogenesis and function. Genes Dev. **18**:357–368.
19. **Li S, et al.** 2005. Requirement for serum response factor for skeletal muscle growth and maturation revealed by tissue-specific gene deletion in mice. Proc. Natl. Acad. Sci. U. S. A. **102**:1082–1087.
20. **Liesa M, et al.** 2008. Mitochondrial fusion is increased by the nuclear coactivator PGC-1β. PLoS One **3**:e3613. doi:10.1371/journal.pone.0003613.
21. **Liesa M, et al.** 2011. Mitochondrial transporter ATP binding cassette mitochondrial erythroid is a novel gene required for cardiac recovery after ischemia/reperfusion. Circulation **124**:806–813.
22. **Lin J, et al.** 2002. Transcriptional co-activator PGC-1α drives the formation of slow-twitch muscle fibres. Nature **418**:797–801.
23. **Little JP, Safdar A, Benton CR, Wright DC.** 2011. Skeletal muscle and beyond: the role of exercise as a mediator of systemic mitochondrial biogenesis. Appl. Physiol. Nutr. Metab. **36**:598–607.
24. **Liu H, et al.** 2007. Yin Yang 1 is a critical regulator of B-cell development. Genes Dev. **21**:1179–1189.
25. **Mootha VK, et al.** 2003. Integrated analysis of protein composition, tissue diversity, and gene regulation in mouse mitochondria. Cell **115**:629–640.
26. **Mootha VK, et al.** 2004. Errα and Gabpa/b specify PGC-1α-dependent oxidative phosphorylation gene expression that is altered in diabetic muscle. Proc. Natl. Acad. Sci. U. S. A. **101**:6570–6575.
27. **Mootha VK, et al.** 2003. PGC-1α-responsive genes involved in oxidative phosphorylation are coordinately downregulated in human diabetes. Nat. Genet. **34**:267–273.
28. **Narkar VA, et al.** 2011. Exercise and PGC-1α-independent synchronization of type I muscle metabolism and vasculature by ERRγ. Cell Metab. **13**:283–293.
29. **Puigserver P, Spiegelman BM.** 2003. Peroxisome proliferator-activated receptor-γ coactivator 1α (PGC-1α): transcriptional coactivator and metabolic regulator. Endocr. Rev. **24**:78–90.
30. **Puigserver P, et al.** 1998. A cold-inducible coactivator of nuclear receptors linked to adaptive thermogenesis. Cell **92**:829–839.
31. **Rezai-Zadeh N, et al.** 2003. Targeted recruitment of a histone H4-specific methyltransferase by the transcription factor YY1. Genes Dev. **17**:1019–1029.
32. **Risson V, et al.** 2009. Muscle inactivation of mTOR causes metabolic and dystrophin defects leading to severe myopathy. J. Cell Biol. **187**:859–874.
33. **Sahin E, et al.** 2011. Telomere dysfunction induces metabolic and mitochondrial compromise. Nature **470**:359–365.
34. **Scarpulla RC.** 2011. Metabolic control of mitochondrial biogenesis through the PGC-1 family regulatory network. Biochim. Biophys. Acta **1813**:1269–1278.
35. **Scarpulla RC.** 2008. Transcriptional paradigms in mammalian mitochondrial biogenesis and function. Physiol. Rev. **88**:611–638.
36. **Schreiber SN, et al.** 2004. The estrogen-related receptor α (ERRα) functions in PPARγ coactivator 1α (PGC-1α)-induced mitochondrial biogenesis. Proc. Natl. Acad. Sci. U. S. A. **101**:6472–6477.
37. **Subramanian A, et al.** 2005. Gene set enrichment analysis: a knowledge-based approach for interpreting genome-wide expression profiles. Proc. Natl. Acad. Sci. U. S. A. **102**:15545–15550.
38. **Tarnopolsky MA, Raha S.** 2005. Mitochondrial myopathies: diagnosis, exercise intolerance, and treatment options. Med. Sci. Sports Exerc. **37**:2086–2093.
39. **Thomas MJ, Seto E.** 1999. Unlocking the mechanisms of transcription factor YY1: are chromatin modifying enzymes the key? Gene **236**:197–208.
40. **Wallace DC, Fan W.** 2009. The pathophysiology of mitochondrial disease as modeled in the mouse. Genes Dev. **23**:1714–1736.
41. **Wallace DC, Fan W, Procaccio V.** 2010. Mitochondrial energetics and therapeutics. Annu. Rev. Pathol. **5**:297–348.
42. **Weill L, Shestakova E, Bonnefoy E.** 2003. Transcription factor YY1 binds to the murine beta interferon promoter and regulates its transcriptional capacity with a dual activator/repressor role. J. Virol. **77**:2903–2914.
43. **Wenz T, Diaz F, Spiegelman BM, Moraes CT.** 2008. Activation of the PPAR/PGC-1α pathway prevents a bioenergetic deficit and effectively improves a mitochondrial myopathy phenotype. Cell Metab. **8**:249–256.
44. **Wenz T, Rossi SG, Rotundo RL, Spiegelman BM, Moraes CT.** 2009. Increased muscle PGC-1α expression protects from sarcopenia and metabolic disease during aging. Proc. Natl. Acad. Sci. U. S. A. **106**:20405–20410.
45. **Wilkinson FH, Park K, Atchison ML.** 2006. Polycomb recruitment to DNA in vivo by the YY1 REPO domain. Proc. Natl. Acad. Sci. U. S. A. **103**:19296–19301.
46. **Wolny S, McFarland R, Chinnery P, Cheetham T.** 2009. Abnormal growth in mitochondrial disease. Acta Paediatr. **98**:553–554.
47. **Wu H, et al.** 2002. Regulation of mitochondrial biogenesis in skeletal muscle by CaMK. Science **296**:349–352.
48. **Wu Z, et al.** 1999. Mechanisms controlling mitochondrial biogenesis and respiration through the thermogenic coactivator PGC-1. Cell **98**:115–124.
49. **Xi H, et al.** 2007. Analysis of overrepresented motifs in human core promoters reveals dual regulatory roles of YY1. Genome Res. **17**:798–806.
50. **Yao YL, Yang WM, Seto E.** 2001. Regulation of transcription factor YY1 by acetylation and deacetylation. Mol. Cell. Biol. **21**:5979–5991.
51. **Ylikallio E, Suomalainen A.** 2012. Mechanisms of mitochondrial diseases. Ann. Med. **44**:41–59.